Environmental Science Nano

PAPER

View Article Online
View Journal | View Issue

Check for updates

Cite this: *Environ. Sci.: Nano*, 2018, 5, 1608

Graphene oxide impairs the pollen performance of *Nicotiana tabacum* and *Corylus avellana* suggesting potential negative effects on the sexual reproduction of seed plants†

Fabio Candotto Carniel, *[a] Davide Gorelli,[b] Emmanuel Flahaut,[c] Lorenzo Fortuna,[a] Cecilia Del Casino,[b] Giampiero Cai,[b] Massimo Nepi,[b] Maurizio Prato[de] and Mauro Tretiach[a]

Received 12th January 2018,
Accepted 26th March 2018

DOI: 10.1039/c8en00052b

rsc.li/es-nano

The production of graphene based materials (GBMs) is steadily increasing but the effects of the possible release of GBMs in the environment are far from being understood. Graphene oxide (GO) is among the most active GBMs and it causes widely varying effects on the vegetative body of seed plants. However, nothing is known yet about its potential effects on the reproductive process. This study addresses the effects of GO on pollen germination and pollen tube elongation in the model species *Nicotiana tabacum* and in the non-model species *Corylus avellana*. *In vitro* germination experiments were conducted without or with GO (control and treated samples, respectively) at concentrations of 25, 50 and 100 μg mL^{-1}. Pollen germination and tube elongation were affected at GO concentrations ≥50 μg mL^{-1}, decreasing by 20% and 19% in *N. tabacum* and by 68% and 58% in *C. avellana*, respectively. GO did not affect the viability of *N. tabacum* pollen, but doubled the frequency of bent tubes. Microscopy observations of pollen tubes exposed to a cell-permeant, dual-excitation ratiometric pH indicator revealed that GO affected the intracellular pH homeostasis. Further germination experiments on *C. avellana* conducted by inverting the pH conditions of the control and treated (100 μg GO mL^{-1}) samples demonstrated that the main factor influencing the pollen performance is the acidic properties of GO. This might affect the reproductive process of numerous seed plants thus being relevant from an environmental point of view.

Environmental significance

The introduction of graphene nanomaterials into the environment is raising concerns on environmental safety. Despite the increasing understanding of the toxic effects of graphene oxide (GO) on photoautotrophic organisms, nothing is known yet concerning the effects on the sexual reproduction of seed plants. We found that *in vitro* exposure to high concentrations of GO impairs the pollen performances of two species, the tobacco plant (*Nicotiana tabacum* L.) and the common hazel (*Corylus avellana* L.), due to the acidic properties of GO. For this reason, the pollen of numerous other plants might exhibit a similar sensitivity to GO. These results raise some concerns for the possible implications in different fields, from crop production to ecosystem functionality.

Introduction

Graphene is "a two-dimensional crystal composed of monolayers of carbon atoms arranged in a honeycombed network with six-membered rings"[1] and is the first 2D material made available.[2] Graphene based materials (GBMs) have attracted wide interest in the last decade because they display extraordinary physical and chemical properties, such as supreme electrical and thermal conductivities and high surface area, clearly distinguishing them from graphite and carbon nanotubes. Therefore, GBMs are expected to be used more often in emerging applications in sectors such as optoelectronics, nanocomposites, biomedicine, energy generation and storage

[a] *Department of Life Sciences, University of Trieste, via L. Giorgieri 10, I-34127 Trieste, Italy. E-mail: fcandotto@units.it; Tel: +0039 0405583879*
[b] *Department of Life Sciences, University of Siena, via P. A. Mattioli 4, I-53100 Siena, Italy*
[c] *CIRIMAT, Université de Toulouse, CNRS, INPT, UPS, UMR CNRS-UPS-INP N° 5085, Université Toulouse 3 Paul Sabatier, Bât. CIRIMAT, 118, route de Narbonne, 31062 Toulouse cedex 9, France*
[d] *Centre of Excellence and Nanostructured Materials (CENMAT), INSTM, unit of Trieste, Department of Chemical and Pharmaceutical Sciences, University of Trieste, via L. Giorgieri 1, I-34127 Trieste, Italy*
[e] *Carbon Nanobiotechnology Laboratory, CIC biomaGUNE, Paseo de Miramón 182, E-20009 Donostia—San Sebastian, Spain*

† Electronic supplementary information (ESI) available: Fig. S1 and S2 and Tables S1–S3. See DOI: 10.1039/c8en00052b

and high sensitivity sensors.[2] The estimated annual production of graphene is around 120 tons[3] but is supposed to increase to 1000 tons by 2019.[4] Estimates for the GBM market foresee investments of almost $400 million by 2025,[5] and industrial patent applications have promptly increased in recent years.[4] Hence, an important part of the applications exploiting GBMs will likely end up in devices and objects of common use increasing the GBM demand. In this regard, GBM inclusion in the rubber of bike tires is already a reality (https://www.vittoria.com/graphene-evidence/),[6] whereas the inclusion in tires for motor vehicles is a patented application.[7] Furthermore, new graphene oxide-Ag composites are being developed to fight crop plant diseases, such as the bacterial leaf blight (*Xanthomonas oryzae* pv. *oryzae*) affecting rice,[8] through aerial applications. The large scale production of GBMs, wearing out of graphene-enriched products, and poor disposal of the derived wastes might result in a significant release and accumulation of GBMs in the environment, as has already happened for other synthetic materials such as plastics.[9,10] Thanks to their dimensions from hundreds of nanometers to a few micrometers and to their extreme lightweight, GBM flakes or nanoparticles might be aero-dispersed as particulate matter with a diameter size $\leq$2.5 μm ($PM_{2.5}$). Once aero-dispersed, $PM_{2.5}$ can be transported for long distances, as reported for carbon black nano-particles,[11] and eventually settle over the vegetation as wet or dry depositions. These premises raise important concerns about possible negative impacts of GBM release on the biota.

So far, widely varying effects (including positive and negative) of GBMs on seed plants have been reported, possibly owing to different experimental conditions (materials, concentrations, exposure time, protocols *etc.*) and/or species tested.[12–15] In general, however, there is agreement on the greater toxicity of graphene oxide (GO) with respect to other GBMs.[16] This is likely due to the high number of oxygen functional groups, such as hydroxyl, carboxyl and epoxy, spread over the graphene lattice which render GO more hydrophilic and reactive towards the surrounding environment.[17] Expectedly, the effects of GBMs on seed plants were always evaluated on the vegetative body at different developmental stages, from seed germination to the flowering adult plants. However, nothing is known yet about the effects of GBMs on the complex, delicate reproductive process, which strongly relies on the transfer and interaction of the male pollen grains with the female reproductive structures. The few-celled pollen grain plays the crucial role of delivering the sperm cells, through the formation of a pollen tube, to the egg cell(s) inside the ovule. If this task is successful, fertilization can occur, with the formation of a new embryo, and later, of a seed. This process is fundamental for the reproduction of almost all seed plants but it is also important for humankind since the yield of crop species, largely consisting of seeds and fruits, relies *in toto* on it. Pollen is more sensitive to environmental pollutants compared to most other structures of the vegetative body of seed plants.[18,19] For this reason, pollen is considered as an experimental model for assessing the impact of a wide variety of chemicals on plant metabolism.[20] It was also used as an indicator of air pollution because the pollen performance, when described in terms of pollen germination and pollen tube elongation, can be affected (depending on species) by gaseous airborne pollutants such as NO_x, O_3 and SO_2.[21–23] More recently, it was demonstrated that also airborne particulate matter affects pollen performance: Speranza *et al.*[24,25] found that Ag- and Pd-nanoparticles impair the *in vitro* pollen germination and the elongation of the pollen tube in the kiwifruit vine, *Actinidia deliciosa* C. F. Liang & A. R. Ferguson. Interestingly, this effect is derived from the nanoparticles themselves rather than from the ions carried on their surface.[24,25] Given these premises, our hypothesis is that the interaction of aero-dispersed GBM flakes with pollen might impair the pollen performances affecting negatively the reproductive process of seed plants. To verify this, the effect of GO, the most reactive GBM tested so far, was verified on the pollen performance of two species, the entomophilous tobacco plant (*Nicotiana tabacum* L.) and the anemophilous common hazel (*Corylus avellana* L.), through *in vitro* germination experiments.

Materials and methods

Graphene oxide preparation and characterization

Graphene oxide (GO) was provided by Grupo Antolin (Burgos, S) within the Graphene Flagship project (http://graphene-flagship.eu/) and it was produced by oxidation of carbon fibers (GANF Helical-Ribbon Carbon Nanofibres, GANF®) in sulfuric acid with sodium nitrate at 0 °C. Dry GO was re-suspended in water and sonicated in an ultrasonic bath prior to the experiments.

The surface chemical composition of GO was analyzed by X-ray photoelectron spectroscopy (XPS) using a Thermoelectron K-α apparatus (ThermoFisher Scientific, MA, USA). The photoelectron emission spectra were recorded using Al-Kα radiation ($h\upsilon$ = 1486.6 eV) from a monochromatized source. The X-ray spot diameter on the sample surface was 400 μm. The pass energy was fixed at 30 eV. The spectrometer energy calibration was performed using the Au $4f^{7/2}$ (83.9 ± 0.1 eV) and Cu $2p^{3/2}$ (932.8 ± 0.1 eV) photoelectron lines. The background signal was removed using the Shirley method.[26] Atomic concentrations were determined from photoelectron peak areas using the atomic sensitivity factors reported by Scofield,[27] taking into account the transmission function of the analyzer. The morphology of the dried particles and their sizes were characterized using a JEM 1400 (Jeol USA, Inc., MA, USA) Transmission Electronic Microscope (TEM) operated at 120 kV, and the GO samples for the observations were prepared according to Garacci *et al.*[28] The GO average flake thickness was assessed by X-ray powder diffraction (XRD) analysis using a D4 ENDEAVOR diffractometer (Bruker Corp., MA, USA) at a wavelength of Cu Kα1 (λ = 0.15418 nm). The GO structure was assessed by Raman spectroscopy using a Labram-HR800 (Horiba Group, J) equipped with a thermoelectrically cooled CCD, using

excitation lasers at 633 (red laser, He/Ne) and 532 nm (green laser, diode-pumped solid-state laser). Five spectra were averaged for each sample and the intensity ratio between the D and the G lines (I_D/I_G) was measured after baseline correction.

Two additional GOs were purchased from Graphenea (San Sebastián, E) and Sigma-Aldrich (St. Louis, MO, USA); they were provided as water suspensions at concentrations of 4 and 2 mg GO mL^{-1}, respectively. Data regarding these materials can be found in the safety datasheets available on the websites of the producers.

Pollen material

The pollen of *Nicotiana tabacum* was collected in the summer of 2016 from dehiscent anthers of plants grown in the experimental fields of the Botanical Garden, University of Siena. Mature undehiscent anthers were sampled, transported to the laboratory and kept at 20 °C until dehiscence. The pollen was gently separated from the anthers and collected in Eppendorf tubes. The pollen of *Corylus avellana* was collected in January 2017 from 15 native trees in the Classical Karst (Trieste, NE Italy) far from pollution sources. Twigs bearing unripe catkins were sampled, immediately transported to the laboratory, and their bases cut under water and kept immersed under laboratory conditions (20 °C, dim light) until flower ripening and stamen dehiscence (c. 48 h). The harvested pollen of both species was sieved through 100 and then 60 μm mesh sizes to remove debris, dehydrated over silica-gel (RH ~5%) for 48 h and stored at −20 °C until use.

Germination of *N. tabacum* and *C. avellana* pollen

Prior to use, the pollen of *N. tabacum* and *C. avellana* was thawed and then rehydrated in a moist chamber for 2 and 3 h, respectively. Germination experiments were performed by suspending the pollen at a concentration of 1 mg mL^{-1} in Brewbaker & Kwack's culture medium[29] (BK) containing 1.62 mM H_3BO_3, 1.25 mM $Ca(N0_3)_2{\cdot}4H_2O$ (or $CaCl_2{\cdot}2H_2O$), 2.97 mM KNO_3 (or KCl) and 1.65 mM $MgSO_4{\cdot}7H_2O$. Germination of *N. tabacum* and *C. avellana* pollen was carried out in BK supplemented with sucrose (BK_{suc}) to a final concentration of 12% and 15% (w/v), respectively.

To assess the effects of GO, the pollen of both species was germinated in BK without GO (control samples), and in BK supplemented with GO suspensions to final concentrations of 25, 50 or 100 μg mL^{-1} (treated samples). Three to four replicates have been prepared for both the control and treated samples. Germination experiments were performed at a controlled temperature of 25 °C. An additional experiment was performed on the *N. tabacum* pollen replacing sucrose with polyethylene glycol (PEG) to a final concentration of 13% (BK_{PEG}).

Assessment of pollen performances

Images of the germinating pollen were taken after 1 and 2 h of pollen tube growth for *N. tabacum* and 3 and 5.5 h for *C. avellana* using a Zeiss Axiocam MRm camera connected to a Zeiss Axiophot microscope (Zeiss, Oberkochen, D). The pollen performance, *i.e.* germination percentage and pollen tube length, was measured on the control and treated samples. The germination percentage was calculated by scoring at least 150 randomly selected grains which were considered germinated if the pollen tube was longer than the average diameter of the pollen grains. The pollen tube length was measured for at least 50 randomly selected pollen tubes. Further measurements ($n > 60$) of the angle made by the pollen tube were taken from the control samples and from the samples treated with GO at 100 μg mL^{-1}.

Viability assay

The viability of *N. tabacum* pollen grains was evaluated in the control and in the treated samples (100 μg mL^{-1} GO only) using the fluorochromatic reaction test.[30] A few drops of fluorescein diacetate solution (2 mg mL^{-1} FDA in acetone) were added to glass slides, waiting 30–40 seconds to allow acetone evaporation.[23] Thereafter, 30 μL of the pollen culture was added to each slide and then covered with coverslips. FDA fluorescence was visualized after 30 min, 1 h and 2 h using a Zeiss Axiophot fluorescence microscope equipped with a Zeiss Axiocam MRn camera; evaluation of viability percentage was done on the captured images by counting at least 150 pollen grains for each sample.

Analysis of pollen tube intracellular pH

The intracellular pH variation along the *N. tabacum* pollen tubes was assessed in the control samples and in the samples treated with GO at 100 μg mL^{-1} using the fluorescent dye BCECF-AM (acetoxymethyl). A BCECF-AM (2,7-bis-(2-carboxyethyl)-5-(e-6)-carboxyfluorescein) ester probe was used to visualize proton levels (*i.e.* pH) in the pollen tubes of *N. tabacum*.[31] A final concentration of 5 μM was obtained from a 1 mM stock solution in dimethyl sulfoxide (DMSO); the required volume was directly added to the germination medium containing resuspended pollen grains. The cytosolic pH was immediately measured after addition of the probe to prevent probe absorption of the organelles (vacuoles). The samples were observed using a Zeiss AxioImager fluorescence microscope equipped with structured illumination in the FITC filter (Ex. λ = 488 nm; Em. λ = 515 nm).

Pollen performances at different pH in relation to GO treatments

The pH of BK_{suc} and BK_{PEG} with or without GO at 100 μg mL^{-1} was measured using a Crison Basic 20 (Crison, Hach Lange, S) pH-meter in continuously stirred media until the variation measured by the probe was less than ±1 mV per minute. The germination performance of the *C. avellana* pollen was evaluated in the pH range between 3 and 7 by incubating the pollen for 3 h in the BK medium adjusted with 0.1 M NaOH or H_2SO_4, as appropriate. Subsequently, the pollen germination performance was further investigated in the

following media: i) BK_{suc} (control), ii) BK_{suc} adjusted with H_2SO_4 to pH 4.2, iii) BK_{suc} with GO at 100 μg mL^{-1} and iv) the latter adjusted with NaOH to pH 6.3. For comparison, the pH of water suspensions (100 μg mL^{-1}) of commercially available GOs, *i.e.* GO from Graphenea (San Sebastián, E), and Sigma-Aldrich (St. Louis, MO, USA), was also measured.

Data analysis

Measurements of pollen performance, tube angles and fluorescence signals from FDA and BCECF-AM were performed using the ImageJ software ver. 1.51J8 (Wayne Rasband, NIH, USA) after calibration of the images with the scalebar command of the Axiovision software (Zeiss, D).

In order to exclude bias due to slow growing pollen tubes or to pollen which stopped growing, only the 30% longest tubes of both the control and treated samples were selected for statistical analyses. The length of selected pollen tubes was expressed as the percentage ratio with respect to the mean tube length measured in the control samples. Factorial ANOVA followed by Tukey's HSD post-hoc test were used to evaluate the statistical differences among the control and treated samples in terms of both pollen germination percentage and pollen tube length using optimal germination times (1 and 2 h for *N. tabacum*; 3 and 5.5. h for *C. avellana*) and GO concentrations (0, 25, 50 and 100 μg mL^{-1}) as the categorical factors. The same statistical analysis was performed for the pH experiment using germination time and pH as the categorical factors. The effect of GO on the pollen tube angle and on the pollen viability was assessed by running a Mann–Whitney U-test for independent samples. All calculations were performed using Microsoft Office Excel 2003 SP3 (Microsoft corporation, WA, USA) and STATISTICA 8.0 (StatSoft Inc., OK, USA).

Results and discussion

Characterization of GO

In the case of the GO sample provided by Grupo Antolin, the elemental analysis data (Table S1†) obtained either by classical chemical analysis (data as provided by Grupo Antolin) or measured experimentally by XPS at the CIRIMAT facility revealed some interesting information. In particular, the C/O ratio, which is often reported in publications, is very sensitive to the input data (weight concentrations or atomic concentrations). If XPS analysis is focused only on the C and O elements, neglecting other elements such as hydrogen which is essentially impossible to detect by this technique, the C/O

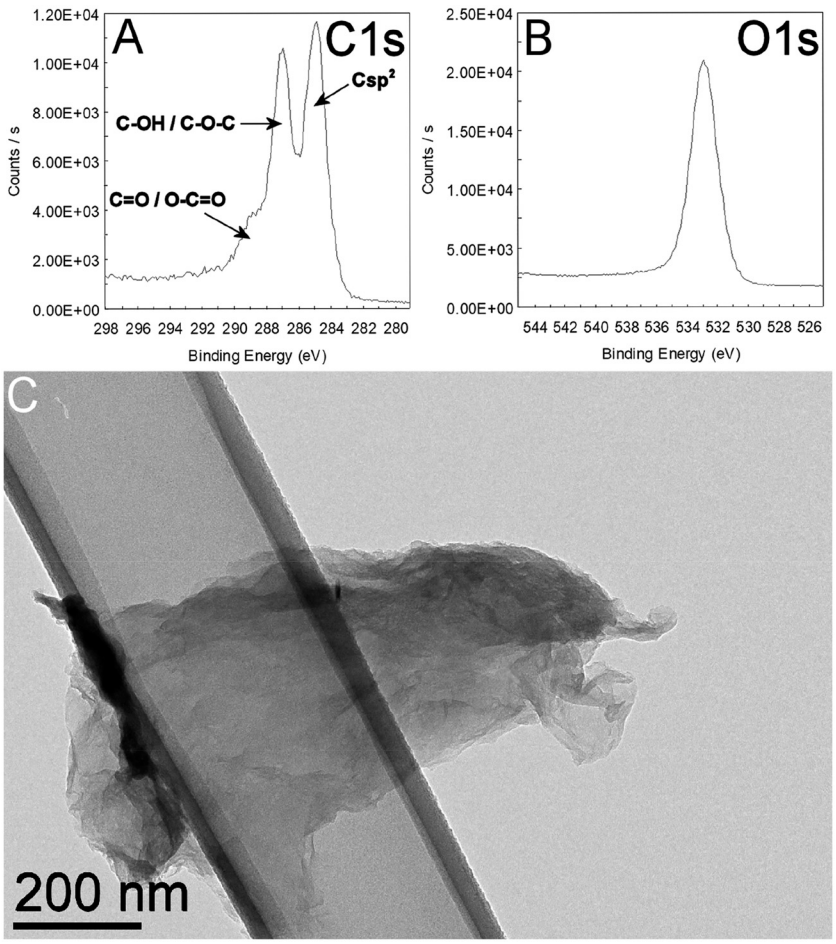

Fig. 1 XPS analysis of GO showing details of the C1s (A) and O1s (B) bands. A typical TEM image of the GO material is shown in (C).

ratio is largely over-evaluated (2.3) while the use of the weight concentrations obtained from the classical chemical elemental analysis leads to a C/O ratio close to 1. This is important to know because in most publications the chemical elemental analysis data are absent; so, it is impossible to know which elements are also present in addition to C and O. In this case, it is obvious that the presence of a high atomic % of hydrogen leads to important differences in terms of C/O ratio depending on considering it or not.

The GO nanoparticles (Fig. 1C) had a thickness of 3.9 nm, calculated using the Scherrer equation applied to the (002) reflection (Fig. S1†) and assuming an interlayer spacing of 0.8 nm obtained from the position of the same reflection (peak at 11.05° of Fig. S1†). These data suggest that the estimated number of layers was between 4 and 5 per particle. The intensity ratios between the D and the G bands (Fig. S2 a and b†) measured by Raman spectroscopy were 1.03 and 1.17 at 532 and 633 nm, respectively, revealing in both cases a rather disordered material.

Physical interaction between GO and the pollen

The *Nicotiana tabacum* pollen germinated in BK_{suc} with GO formed clusters intermingled with GO flakes especially at the highest concentration (100 μg mL^{-1}; Fig. 2A and B), which made the measurements of pollen performance unreliable (n. a. data in Fig. 3A and C). Interestingly, the replacement of sucrose with PEG reduced the aggregation effect allowing the measurements (Fig. 2B and C and 3B and D). Such pollen-GO clusters were not observed in *C. avellana* germinated under the same conditions (Fig. 2D). In any case, GO flakes were found adhering to the pollen grains and the pollen tube surfaces in both species (Fig. 2D and E). The pollen grains of *N. tabacum* are generally coated by a lipoid "pollen coat" or "pollenkitt" which can account for 10–15% of the total pollen mass.[32,33] This coat is typical of entomophilous species: it has adhesive properties allowing pollen grains to stick to insects and to the stigmatic surfaces of flowers.[34] Moreover, the germinating pollen grains of *N. tabacum* release lectins and polylectins, which may also cause grain agglutination.[33] Both may explain the pollen-GO aggregation and why this did not occur in the anemophilous *C. avellana*. As reported by Chen *et al.*,[35] PEG has a good affinity to lipoid substances, and therefore it might have partially removed the pollen coat reducing the aggregation between the pollen and GO.

Effect of GO on pollen performances and viability

The pollen of *N. tabacum* and *C. avellana* germinated in BK_{suc} (control samples) had normal tube extrusion and elongation (Fig. 2A) with final germinations of 75% and 81% (Fig. 3A and 4A), respectively, suggesting that the pollen materials were healthy at the beginning of the experiments. The pollen performance of both species was significantly affected by GO (see Tables S2 and S3†). The pollen germination and tube length of *N. tabacum* decreased to 55% and 81% with respect to the control values (Fig. 3B and D; $P < 0.05$), respectively, after 2 h of germination at 100 μg GO mL^{-1}. The decrease in pollen performance was greater in *C. avellana*; the germination remained steady

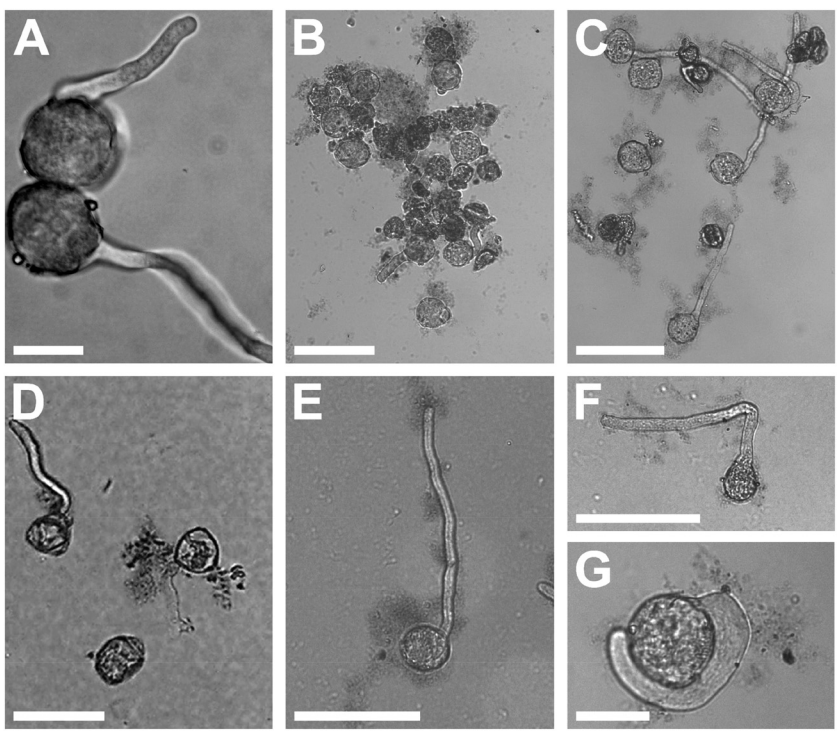

Fig. 2 Pollen of *N. tabacum* in BK_{PEG} after 1 h (A), BK_{suc} (B) or BK_{PEG} (C) at 100 μg GO mL^{-1} after 2 h. Pollen of *C. avellana* in BK_{suc} at 50 μg GO mL^{-1} after 5.5 h (D). Straight (E) or bent (F and G) grown pollen tubes of *N. tabacum* at 100 μg GO mL^{-1}. Bars: A, G = 20 μm; D = 50 μm; B, C, E, F = 100 μm.

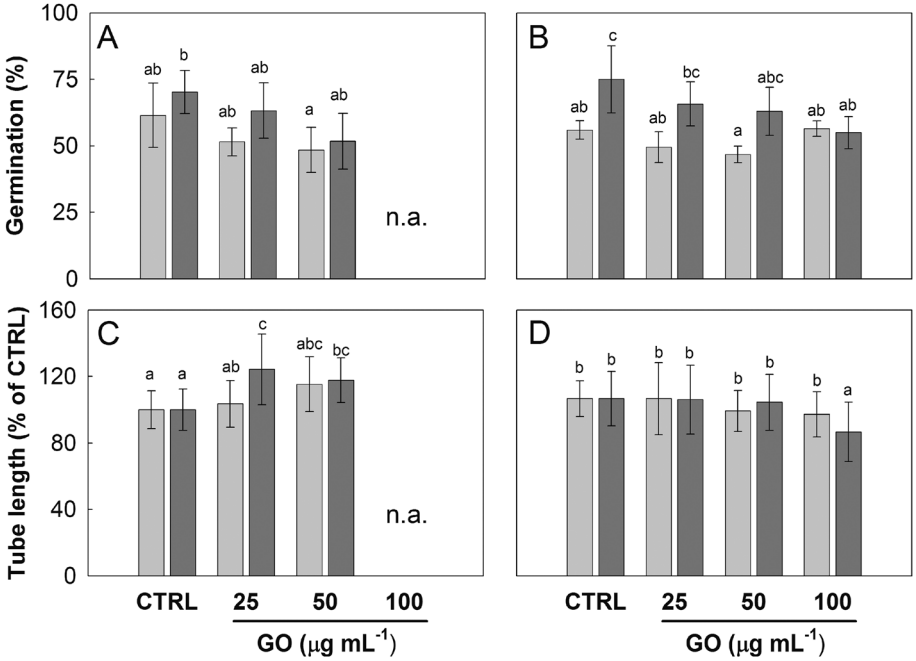

Fig. 3 Germination percentage (A and B) and pollen tube growth (C and D) measured in *Nicotiana tabacum*. Pollen germinated in BK_{suc} (A and C) or BK_{PEG} (B and D) without (CTRL) or with 25, 50 or 100 μg GO mL^{-1} after 1 h (grey bars) and 2 h (dark grey bars). Values are reported as means ±1 st. dev. (n = 150 for A and C; $n \geq 50$ for C and D). Statistically different groups are marked with different letters (two-way ANOVA, Tukey's HSD post-hoc test). n.a. = not available data.

until 50 μg GO mL^{-1}, then it decreased to 12% and 14% at 100 μg mL^{-1} after 3 and 5.5 h, respectively (Fig. 4A). Differently, the pollen tube length decreased progressively with the increase in GO concentration, reaching 62% and 43% of the control value at 100 μg GO mL^{-1} after 3 and 5.5 h, respectively (Fig. 4B). Furthermore, although the viability of the *N. tabacum* pollen was not affected at 100 μg GO mL^{-1} (Fig. 5), the percentage of pollen tubes showing a bent growth doubled with respect to that of the control samples (Fig. 6; $P < 0.05$). A similar trend was observed in the pollen tubes of *C. avellana*, but the difference between the control and treated samples was not statistically significant (Fig. 6). The fact that GO had an effect on the pollen performance of both species, although with a different intensity, agrees well with the literature reporting the toxic effects of GO on phylogenetically unrelated model organisms.[16] However, the mechanisms of toxicity are still unclear: some authors reported that GO can mechanically damage cells or tissues with its sharp edges[36] and reduce metabolic activity and viability when it is internalized into cells.[37,38] The great majority, though, agrees that GO causes oxidative stress inducing the formation of reactive oxygen species.[39–41] In our case, the observed effects are mostly related to the GO composition in terms of functional groups and their interaction with the surrounding media, as it will be discussed below.

Effect of GO on the pH of germination media

Graphene oxide is characterized by a high number of functional groups containing oxygen, with hydroxyl and epoxy groups spread over the graphene lattice, and carboxyl groups at the flake edges.[17] Carboxyl groups are weak acids and together with hydroxyl groups deprotonate in water solutions lowering the pH. Furthermore, GO could still have some

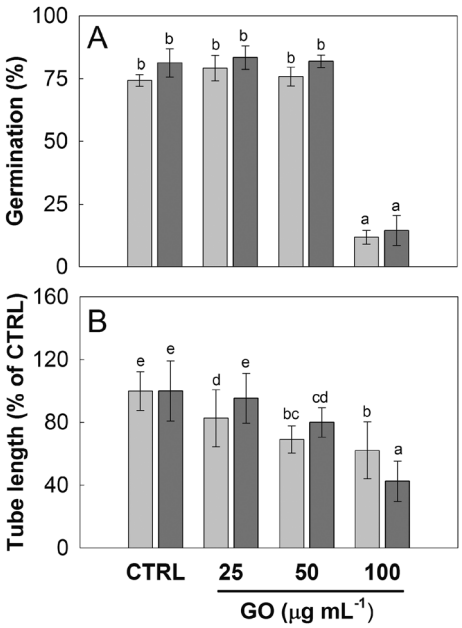

Fig. 4 Germination percentage (A) and pollen tube length (B) measured in *Corylus avellana*. Pollen germinated in BK_{suc} without (CTRL) or with 25, 50 or 100 μg GO mL^{-1} after 3 h (grey bars) and 5.5 h (dark grey bars). Values are reported as means ± 1 st. dev (n = 150 for A; $n \geq 50$ for B). Statistically different groups are marked with different letters (two way ANOVA, Tukey's HSD post-hoc test).

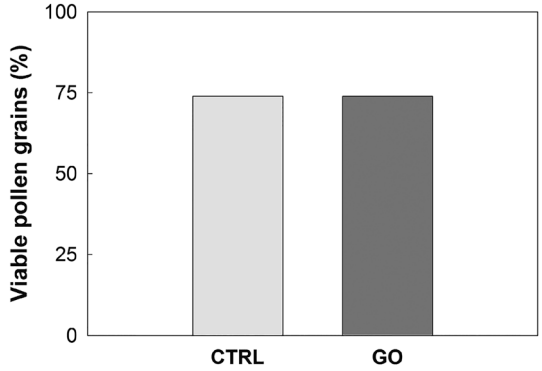

Fig. 5 Percentage of *N. tabacum* viable pollen grains (n = 150) in the control (CTRL) and treated samples with GO at 100 μg mL^{-1} (GO) after 2 h of germination.

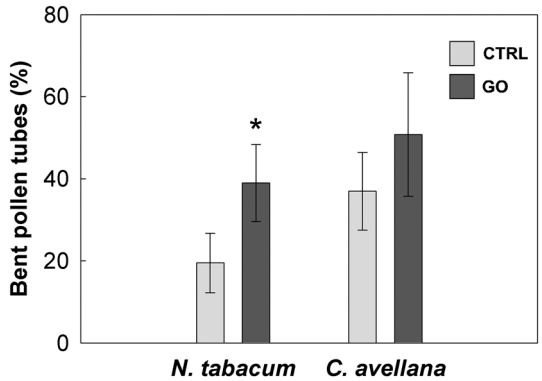

Fig. 6 Percentage of bent pollen tubes in the control (CTRL) and treated samples (100 μg mL^{-1} GO) of *N. tabacum* and *C. avellana* germinated for 2 h and 5.5 h, respectively. Values are means ± 1 st. dev. ($n > 60$); statistical differences between CTRL and GO are marked with an asterisk for $P < 0.05$ (Mann Whitney U-test).

residual sulfuric acid (as suggested by the elemental composition in Table S1†), which is used in the modified Hummers' method for the oxidation process of the graphite flakes.[42] For these reasons, the pH of the BK media and water suspensions of GO of different origins was investigated (Table 1). At 100 μg GO mL^{-1}, the pH of BK_{suc} and BK_{PEG} decreased by 2.00 and 0.97 points, respectively (Table 1). Water suspensions of GO, GO washed to remove potential impurities from the Hummer's method, GO from Graphenea and GO from Sigma-Aldrich had pH values below 4.25 (Table 1), confirming (a) the strong acidic property of all tested GOs, and (b) the negligible sulphuric acid contamination, because the washing of GO did not change the final pH value.

Effect of pH on pollen performances

Considering the strong acidification effect of GO on the BK_{suc} media, we further investigated the effect of pH on the pollen performance of *N. tabacum* and *C. avellana*. As reported by Tupí and Říhová,[43] the *N. tabacum* pollen tube growth has its optimum in the pH range of 5–6.5 and decreases at lower pH (Fig. 7A). The *Corylus avellana* pollen had the best performance at pH 7 with 84% of germinated pollen and an average tube length of 100.4 μm after 3 h of germination (Fig. 7B). Below pH 7, pollen germination slightly decreased to 78% at pH 5–6, fell to 40% at pH 4 and zeroed at pH 3 (Fig. 7B). Differently, the pollen tube length progressively decreased to 73.9 μm at pH 6 and then to 57.9 μm at pH 4 (Fig. 7B). These results help to clarify the contribution of different "toxicity" mechanisms, direct or not, on the performance of *N. tabacum* and *C. avellana* pollen germinated in GO-enriched media (Fig. 3). In the first case, PEG decreased the GO-dependent acidification stabilizing the pH to 5.9, which falls in the pH range where the *N. tabacum* pollen performance is purportedly the best (see Table 1 and Fig. 7A). For this reason, the GO-induced pH change does not explain the decrease in pollen performance detected in *N. tabacum*,

Table 1 pH of the BK media (BK_{suc}, BK_{PEG}) without or with GO (Grupo Antolìn) and pH of dH_2O with GO, GO washed in dH_2O to remove residues of the production method (GO^{w}), GO commercialized by Graphenea (GO§) and Sigma-Aldrich (GO$^{\#}$) at a concentration of 100 μg mL^{-1}. Values are reported as means ± 1 st. dev. (n = 3)

	pH
BK_{suc}	6.36 ± 0.10
BK_{PEG}	6.91 ± 0.02
BK_{suc} + GO	4.35 ± 0.20
BK_{PEG} + GO	5.94 ± 0.10
dH_2O + GO	4.13 ± 0.05
dH_2O + GO^{w}	4.25 ± 0.10
dH_2O + GO§	3.34 ± 0.02
dH_2O + GO$^{\#}$	4.01 ± 0.18

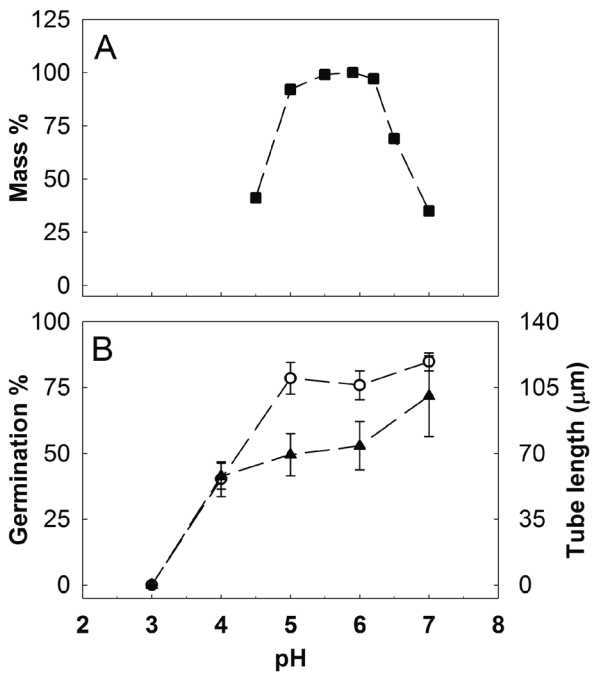

Fig. 7 Percentage of pollen tube mass development in *N. tabacum* [redrawn from Tupí and Říhová (1984)] (A) and germination percentage (-○-) and pollen tube length (-▲-) of *Corylus avellana* (B) as a function of pH. Values in B are means ± 1 st. dev (n = 450 in A; n = 90 in B).

suggesting a different type of interaction between pollen grains and tubes. Inhibition of pollen germination induced by Ag-nanoparticles has already been documented by Speranza *et al.*,[25] who hypothesized a possible physical blockage of the transmembrane ion channels at the site of tube protrusion by the nanoparticles, preventing the formation of the inward ion current preceding pollen germination.[44] Alternatively, GO internalization at the site of the tube protrusion could have impaired the metabolic pathways triggering pollen germination. Further experiments on GBM internalization and GO-induced ROS production are currently ongoing to clarify the mechanisms on the basis of this germination inhibition. The reduction of the pollen tube length by GO can instead be explained, thanks to microscopy observations of GO treated samples stained with BCECF-AM, a fluorescent dye used to detect intracellular changes in pH.[31] The treated pollen suffered a pH variation along their pollen tubes. Fig. 8C and D show a pollen tube covered by GO flakes with regions emitting fluorescence at an intensity of up to two fold higher than that detected in the control samples (Fig. 8B *vs.* E). This certainly affects tube growth and tube directionality because low intracellular pH impairs the cytoskeleton[45] which in pollen tubes coordinates the movements of organelles[46] and vesicle trafficking needed to deposit new pectin at the tube tip for its growth.[47,48] For this reason, localized pH decreases could also explain the higher percentage of bent pollen tubes observed in *N. tabacum* (Fig. 6).

In the case of *C. avellana* instead, GO lowered the pH of BK_{suc} to 4.35, *i.e.* the pH value at which the germination performances of *C. avellana* are the lowest (see Table 1 and Fig. 7B). To verify if the GO-dependent acidification was the main reason for the observed effects, a further experiment was performed, reversing the pH conditions of the media: those of the controls were acidified to pH 4.2, whereas those with GO were adjusted to pH 6.3. The acidified controls decreased similarly to GO-treated samples after both 3 and 5.5 h (Fig. 9) and, conversely, the adjusted GO-treated samples had a pollen performance similar to that of the pristine controls (Fig. 9). These results confirm that GO-induced acidification of the media is the main toxicity mechanism (for P = 0.000, see Table S4†), causing the impairment of pollen performance in *C. avellana*.

The pH-decrease induced by high concentrations of GO might impair the pollen performance of a broad number of seed plants. For instance, Cox[49] tested the pollen performances of 13 forest species over a pH range from 2.6 to 5.6,

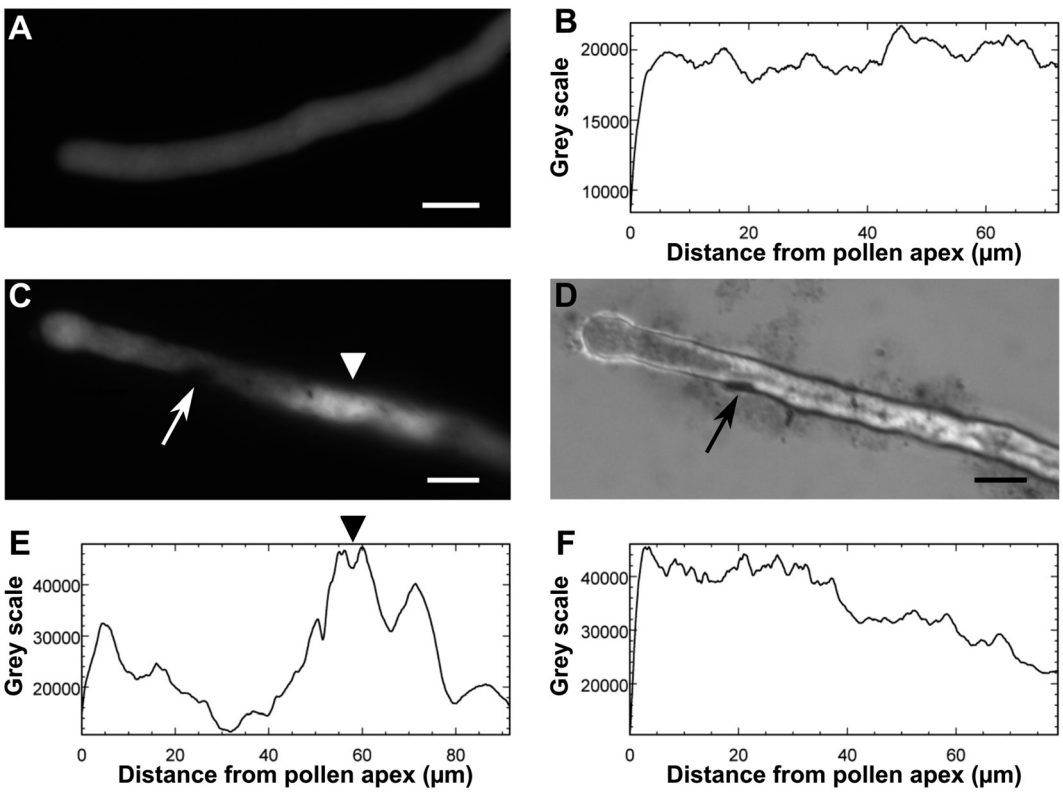

Fig. 8 Variation of the pollen tube pH in germinated *Nicotiana tabacum* L. pollen without or with GO at 100 μg mL^{-1}. The pollen tube from a CTRL sample stained with BCECF-AM and observed by fluorescence microscopy after 2 h of germination (A) and the fluorescence profile of the internalized dye measured along the same pollen tube (B). A pollen tube stained with BCECF-AM from a sample treated with GO and observed by fluorescence (C) and light (D) microscopy after 2 h of germination, and the fluorescence profile of BCECF measured along the same pollen tube of figure C (E) and in the pollen tube of samples treated with GO for 1 h (F). The arrows in C and D indicate GO flakes adhering to the pollen tube, whereas the arrowheads in C and E indicate the maximum of BCECF fluorescence in reference to the distance from the pollen tube apex, respectively. Bars = 10 μm.

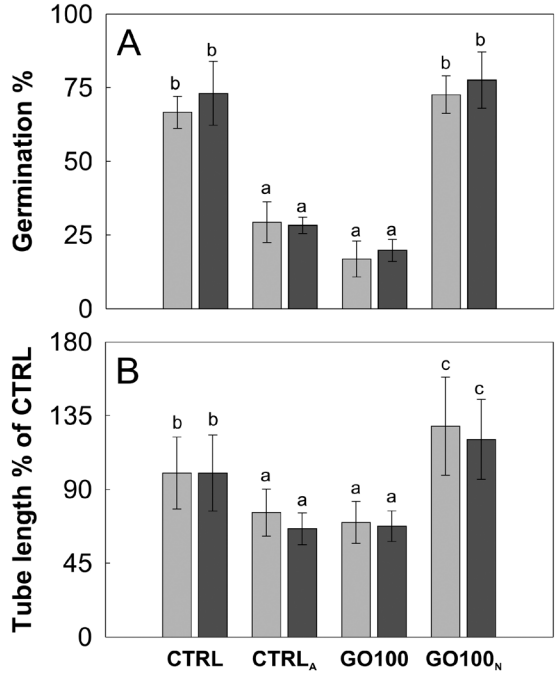

Fig. 9 Germination percentage (A) and pollen tube growth (B) in *Corylus avellana* in BK_{suc} (CTRL) or in BK_{suc} acidified to pH 4.2 ($CTRL_A$) and in BK_{suc} with GO at 100 μg mL^{-1} (GO100) or in GO100 neutralized to pH 6.3 ($GO100_N$). Measurements were taken after 3 (grey bars) and 5.5 h (dark grey bars). Values are reported as means ± 1 st. dev. (n = 450 in A; n = 90 in B). Statistically different groups are marked with different letters for $P < 0.05$ (two-way ANOVA, Tukey's HSD post-hoc test).

simulating the effect of acid rains on the reproductive process of seed plants. He found that in half of the species, the pollen performance was strongly reduced at pH 3.6.

Conclusions and environmental relevance

Aero-dispersed GBM flakes and their environmental fate is still an under-studied field. However, graphene flakes were detected in the air of small-scale graphene manufacturing workplaces (a laboratory and a research institution) in which careful measures to protect operators were adopted.[50] This demonstrates the high volatility of GBMs and raises concerns on the possible release of GBMs that will occur inside and around large scale-production facilities or when these materials are used in degradable objects. For these reasons, in this work, we started addressing the potential effects of GO, one of the most studied and potentially toxic GBMs, on the reproductive process of seed plants by *in vitro* experiments of pollen germination hypothesizing important future releases of GBMs from both point and widespread sources. We showed that GO impaired the pollen performance in *N. tabacum* and *C. avellana* at the highest concentration tested and most of this is derived from the acidic properties of the material. This could be relevant from an environmental point of view because strong depositions of GO flakes on the stigmatic surfaces of angiosperms could decrease pH to a level overcoming the buffering capacities of the organ. Pollen landing on an acidified stigma could be affected and consequently have reduced chances to successfully conclude the reproductive process, as already showed by Cox[49] in connection with the devastating phenomena of acid rains.[51] Furthermore, our experiments brought evidence of another effect of GO, potentially not related to the acidic properties but still important since it reduced the germination performance of *N. tabacum* by 20%, and doubled the frequency of bent tubes. Still unknown in its nature, this might be related to intracellular ROS development or to a perturbation of Ca^{2+} availability, since this ion plays a fundamental role in pollen tube growth.[44] There are no doubts that more experiments involving other GBMs and seed plants, especially of economic value such as cereals, need to be conducted to clarify the mechanisms inducing this effect and its selectivity towards diverse species. It has to be noted though, that the scenario depicted here could be far more complex. Hypothetically, GO flakes deposited on the receptive surface could also affect the reproductive process in other ways, such as reducing the capacity of the stigma to intercept pollen in anemophilous species or hindering physically or chemically the signalling occurring between the stigma and the pollen grain. Also, sexual reproduction of entomophilous seed plants relies on insects for pollination which could collect GO flakes from flower organs or even eat them if the flakes land over nectar or water drops or over the pollen in the open anthers, entering *de facto* in other trophic chains. Furthermore, the effect of GO and other airborne metallic nanoparticles could be amplified by synergistic effects such as those reported by Tang *et al.*[52] in the cyanobacterium *Microcystis aeruginosa*.

Conflicts of interest

The authors declare no competing financial interests.

Acknowledgements

We gratefully acknowledge financial support from the European Union's Horizon 2020 Research and Innovation Programme under grant agreement No. 696656 Graphene Flagship CORE 1. The authors thank Prof. Johanna Wagner (University of Innsbruck) for training FCC in germinating pollen *in vitro*, Dr. Alice Montagner for her valuable help in graphene handling and Drs. Susanna Bosi and Zois Syrgiannis (University of Trieste) for their technical advices. We are indebted to Ilaria Corsi (University of Siena) for the discussion and suggestions about planning of the experimental procedures. The personnel of the Botanical Garden of the University of Siena are also acknowledged for cultivating the plants of *Nicotiana tabacum.* Prof. Ester Vázquez Fernández–Pacheco is thanked for providing washed and non-washed GO materials. P. Lonchambon and G. Chimowa are acknowledged for their help with the physico-chemical characterization of the Antolin GO material.

References

1 A. K. Geim, *Science*, 2009, **324**, 1530–1534.
2 K. S. Novoselov, V. I. Fal'ko, L. Colombo, P. R. Gellert, G. M. Schwab and K. Kim, *Nature*, 2012, **490**, 192–199.
3 R. Ciriminna, N. Zhang, M. Q. Yang, F. Meneguzzo, Y. J. Xu and M. Pagliaro, *Chem. Commun.*, 2015, **51**, 7090–7095.
4 A. Zurutuza and C. Marinelli, *Nat. Nanotechnol.*, 2014, **9**, 730–734.
5 K. Ghaffarzadeh, *Graphene 2D Materials and Carbon Nanotubes: Markets Technologies and Opportunities 2016–2026*, 2016, http://idtechexcom/research/reports/graphene-2d-materials-and-carbon-nanotubes-markets-technologiesand-opportunities-2015-2025-000440asp?viewopt=desc (accessed 02.2010).
6 Vittoria © 2018, *Graphene, Join the revolution*, https://www.vittoria.com/graphene-evidence/ Accessed the (02.2018).
7 A. Zhamu and B. Z. Jang, *US Pat.*, No. 7999027, U.S. Patent and Trademark Office, Washington, DC, 2011.
8 Y. Liang, D. Yang and J. Cui, *New J. Chem.*, 2017, **41**, 13692–13699.
9 M. Cole, P. Lindeque, C. Halsband and T. S. Galloway, *Mar. Pollut. Bull.*, 2011, **62**, 2588–2597.
10 C. M. Rillig, *Environ. Sci. Technol.*, 2012, **46**, 6453–6454.
11 V. Ramanathan and G. Carmichael, *Nat. Geosci.*, 2008, **1**, 221–227.
12 P. Begum, R. Ikhtiari and B. Fugetsu, *Carbon*, 2011, **49**, 3907–3919.
13 N. A. Anjum, N. Singh, M. K. Singh, Z. A. Shah, A. C. Duarte, E. Pereira and I. Ahmad, *J. Nanopart. Res.*, 2013, **15**, 1770.
14 P. Begum and B. Fugetsu, *J. Hazard. Mater.*, 2013, **260**, 1032–1041.
15 Q. Wang, S. Zhao, Y. Zhao, Q. Rui and D. Wang, *RSC Adv.*, 2014, **4**, 60891–60901.
16 A. Montagner, S. Bosi, E. Tenori, M. Bidussi, A. A. Alshatwi, M. Tretiach, M. Prato and Z. Syrgiannis, *2D Mater.*, 2017, **4**, 012001.
17 D. R. Dreyer, S. Park, C. W. Bielawski and R. S. Ruoff, *Chem. Soc. Rev.*, 2010, **39**, 228–240.
18 S. R. Varshney and C. K. Varshney, *Environ. Pollut., Ser. A*, 1980, **24**, 87–92.
19 G. L. Calzoni, F. Antognoni, E. Pari, P. Fonti, A. Gnes and A. Speranza, *Environ. Pollut.*, 2007, **149**, 239–245.
20 U. Kristen, *Toxicol. In Vitro*, 1997, **11**, 181–191.
21 W. Flückiger, S. Braun and J. J. Oertli, *Environ. Pollut.*, 1978, **16**, 73–80.
22 T. Keller and H. Beda, *Environ. Pollut., Ser. A*, 1984, **33**, 237–243.
23 E. Gottardini, F. Cristofolini, E. Paoletti, P. Lazzeri and G. Pepponi, *J. Atmos. Chem.*, 2004, **49**, 149–159.
24 A. Speranza, K. Leopold, M. Maier, A. R. Taddei and V. Scoccianti, *Environ. Pollut.*, 2010, **158**, 873–882.
25 A. Speranza, R. Crinelli, V. Scoccianti, A. R. Taddei, M. Iacobucci, P. Bhattacharya and P. C. Ke, *Environ. Pollut.*, 2013, **179**, 258–267.
26 D. A. Shirley, *Phys. Rev. B: Solid State*, 1972, **5**, 4709–4714.
27 J. H. Scofield, *J. Electron Spectrosc. Relat. Phenom.*, 1976, **8**, 129–137.
28 M. Garacci, M. Barret, F. Mouchet, C. Sarrieu, P. Lonchambon, E. Flahaut, L. Gauthier, J. Silvestre and E. Pinelli, *Carbon*, 2017, **113**, 139–150.
29 J. L. Brewbaker and B. H. Kwack, *Am. J. Bot.*, 1963, **50**, 859–865.
30 J. Heslop-Harrison, Y. Heslop-Harrison and K. R. Shivanna, *Theor. Appl. Genet.*, 1984, **67**, 367–375.
31 H. Qu, X. Jiang, Z. Shi, L. Liu and S. Zhang, *J. Plant Res.*, 2012, **125**, 185–195.
32 P. Piffanelli, J. H. E. Ross and D. J. Murphy, *Plant J.*, 1997, **11**, 549–652.
33 N. P. Matveeva, E. A. Lazareva, T. P. Klyushnik, S. A. Zozulya and I. P. Ermakov, *Russ. J. Plant Physiol.*, 2007, **54**, 619–625.
34 E. Pacini and M. Hesse, *Flora*, 2005, **200**, 399–415.
35 J. Chen, S. K. Spear, J. G. Huddleston and R. D. Rogers, *Green Chem.*, 2005, **7**, 64–82.
36 R. G. Combarros, S. Collado and M. Díaz, *J. Hazard. Mater.*, 2016, **310**, 246–252.
37 F. Ahmed and D. F. Rodrigues, *J. Hazard. Mater.*, 2013, **256**, 33–39.
38 S. Ouyang, X. Hu and Q. Zhou, *ACS Appl. Mater. Interfaces*, 2015, **7**, 18104–18112.
39 K. M. Garza, K. F. Soto and L. E. Murr, *Int. J. Nanomed.*, 2008, **3**, 83–94.
40 S. Liu, T. H. Zeng, M. Hofmann, E. Burcombe, J. Wei, R. Jiang, J. Kong and Y. Chen, *ACS Nano*, 2011, **5**, 6971.
41 W. Zhang, C. Wang, Z. Li, Z. Lu, Y. Li, J. Yin, Y. Zhou, X. Gao, Y. Fang, G. Nie and Y. Zhao, *Adv. Mater.*, 2012, **24**, 5391–5397.
42 D. C. Marcano, D. V. Kosynkin, J. M. Berlin, A. Sinitskii, Z. Sun, A. Slesarev, L. B. Alemany, W. Lu and J. M. Tour, *ACS Nano*, 2010, **4**, 4806–4814.
43 J. Tupí and L. Říhová, *J. Plant Physiol.*, 1984, **115**, 1–10.
44 J. A. Feijó, R. Malhó and G. Obermeyer, *Protoplasma*, 1995, **187**, 155–167.
45 A. H. Timme, *J. Ultrastruct. Res.*, 1981, **77**, 199–209.
46 G. Cai and M. Cresti, *J. Exp. Bot.*, 2009, **60**, 495–508.
47 E. M. Lord and S. D. Russell, *Annu. Rev. Cell Dev. Biol.*, 2002, **18**, 81–105.
48 G. Cai, C. Faleri, C. Del Casino, A. M. Emons and M. Cresti, *Plant Physiol.*, 2011, **155**, 1169–1190.
49 R. M. Cox, *New Phytol.*, 1983, **95**, 269–276.
50 J. H. Lee, J. H. Han, J. H. Kim, B. Kim, D. Bello, J. K. Kim and E. M. Faustman, *Inhalation Toxicol.*, 2016, **28**, 281–291.
51 N. Van Breemen, P. A. Burrough, E. V. Velthorst, H. F. Van Dobben, T. de Wit, T. D. Ridder and H. F. R. Reijnders, *Nature*, 1982, **299**, 548–550.
52 Y. Tang, J. Tian, S. Li, C. Xue, Z. Xue, D. Yin and S. Yu, *Sci. Total Environ.*, 2015, **532**, 154–161.